Chapter 1

Introduction

Chapter 1 presents the introduction of metamaterials and their history, classification, and theory, and a discussion of various applications of metamaterials. The chapter also discusses current research in metamaterial absorbers and related applications in the different frequency regions. The details of the different simulation tools and used modeling software for the analysis of the result are also discussed in this chapter. The motivation related to thesis work is discussed at the end of the chapter.

1.1 Natural materials and Metamaterials

Natural materials typically consist of an assortment of separate atoms and molecules that are bonded together chemically. Three separate phenomena are produced when light (or electromagnetic radiation) interacts with natural materials: First, some of the solar energy that strikes a substance is said to be "absorbed." Second, a portion of these radiations that are not absorbed by the materials is "reflected" back to the environment or atmosphere by the contact medium, which is known as the "Reflection phenomenon." Finally, the transmittance coefficient refers to the portion of the radiation that is neither absorbed nor reflected. Natural substances' absorption, reflection, and transmission properties are determined by their atomic/molecular features.

A non-natural sub-wavelength material known as "metamaterials (MTM)" has recently generated great interest in the development of electromagnetic-based materials because they can exhibit extraordinary electromagnetic properties that are impossible to find in nature and are different from traditional materials. The idea of metamaterials stems from the replacement of man-made materials with natural ones that are much smaller than the wavelengths of light emitted. The degree of finesse in fabrication (geometry, shape, orientation, and size) gives MTM its interesting properties; Its chemical makeup has little effect.

1.2 History of metamaterials

Five decades after the Second World War, metamaterials started to appear. The earliest investigations on the geometry of twisted constructions were done by Jagadis at the end of the nineteenth century (1898), paving the way for the development of synthetic materials[1]. It was originally a synthetic element known as chiral, as modern researchers refer to it. Lindell et al.[2] produced chiral media in the early 20th century (1914) by introducing

numerous randomly oriented tiny wire helices in a host medium. Kock[3] created a lightweight microwave lens in 1948 by manipulating conducting spheres, and the period strips, and modifying the effective refractive index of artificial media. More synthetic materials with unusual properties have been developed as a result of advancements in materials science. Using the photon of light, photonic materials have been produced, leading to the production of photonic crystals[4], based on the experiment carried out by Lord Rayleigh in 1887. The prestigious discovery was made in 1968, however, when Veselago[5] theoretically investigated both negative magnetic permeability (μ) and dielectric permittivity (ε). In his study, he discovered that when traveling through a medium (material) of simultaneously negative ε and μ, the group velocity (v_g) of the given monochromatic plane wave propagates in the direction opposite the energy flux (Poynting vector), as opposed to conventional material, where the v_g always propagates in a direction parallel to Poynting vector.

Naturally, group velocity or chromatic dispersion is highly influenced by the magnetic permeability and electrical permittivity of the material (medium) through which it travels. Vaselago[5] proposed three theories to investigate the remarkable behavior of materials with simultaneously negative permittivity (ε) and permeability (μ). First, he thought that a material's properties would not change even if the signs of ε and μ changed simultaneously. Second, he also believed that the existence of elements with negative μ and ε might be contrary to the basic laws of nature (physics). Third, he conceded that there might have been some attributes that were different from those of positive properties if materials with simultaneously negative (ε and μ) properties exist. Vaselego's hypothesis had to wait a few decades because of this mysterious concept until Smith et al.[6] constructed and verified the existence of the first material with both negative ε and μ in 1999. Smith and his colleagues also predicted the occurrence of a negative refractive index (n) in their

research, which was later explained by the University of Cambridge Professor, Sir Pendry[7]. Following these findings, several research teams have focused on diverse applications in this field. Several papers have been published on MTM for applications in the microwave, infrared (IR), terahertz, and optical spectrum regimes of light.

1.3 Classifications of materials

Electromagnetic (EM) qualities such as electric permittivity (ε) and magnetic permeability (μ) have a significant impact on the interaction between material and EM wave (light). Typically, the propagation of EM waves in a medium is greatly influenced by magnetic permeability and electric permittivity. This is because the dispersion equation[5] only contains these two parameters. The following dispersion relations can be used to show how the electric permittivity governs the interaction between an applied electric field and the contacting medium, while the magnetic permeability dictates how the material responds to an applied magnetic field.

$$k = \omega\sqrt{\mu\varepsilon} \tag{1.1}$$

Where, ω and k represent the frequency and wavenumber of an electromagnetic wave, respectively.

The relationship Eq. 1.1 between the index of refraction (n), wave vectors, and angular frequency can be translated into Eqs. 1.2 and 1.3 respectively.

$$n = \sqrt{\mu\varepsilon} \tag{1.2}$$

$$n = \frac{k}{\omega} \tag{1.3}$$

Changing the sign of ε and μ does not affect these equations, as shown by relations Eqs. 1.1 and 1.2. Vaselago[5] described this by noting that if the signs change but have no influence on Eqs. 1.1 and 1.2, materials with both negative permeabilities (μ) and permittivity (ε) may not exist, or even if they do, they must have unique qualities that set them apart from more common materials.

Most electromagnetic materials[8] can be easily identified by the quadrant in which they lie in the ε and μ plane, as shown in Fig. 1.1:

I. A material or medium in which monochromatic waves travel in a conventional path and obey Snell's law[9] of refraction is the first 'Right-handed materials' substance. In other words, a double positive media (DPM) is a medium that contains most of the dielectric and has both positive permittivity ($\varepsilon(\omega)>1$) and permeability $\mu(\omega)>1$). The right-hand rule is observed in right-handed materials by the wave vector (k), electric field (E), and magnetic field (H).

II. A μ-negative (MNG) medium has a permittivity greater than zero ($\varepsilon(\omega)>1$) and a permeability less than zero ($\mu(\omega)<1$). A wave impacting this type of medium decays evanescently within the medium, and no propagating modes can be sustained. There can be no exact analog of an electric plasma due to the lack of magnetic monopoles, however, there are natural instances of various anti-ferromagnetic and ferri-magnetic materials with a microwave resonance that display $Re(\mu)<0$ within a frequency band above the resonance frequency.

III. Vaselago[5] proposed the idea of "Left-handed material", which is defined as a substance or medium in which monochromatic waves propagate in an unusual direction, resulting in negative signals of ε and μ in that medium. The Poynting vector and wave vector move in opposite directions in such a medium. For better

understanding, we can understand in this way that a double negative (DNG) medium has a positive permeability and a permeability that is less than zero ($\varepsilon(\omega)<1$ & $\mu(\omega)<1$). For better understanding, we can understand this way that a double negative (DNG) medium has less than zero negative permeability ($\varepsilon(\omega)<1$) and less than zero negative permeability ($\mu(\omega)<1$). Only artificial creations have been used to demonstrate this class of materials. Backward wave propagation is observed in such a material, which is also known as a Left-handed medium[8]. The transverse electromagnetic wave propagates with a phase velocity of c/n (where n is the refractive index), and the propagation constant (k) for DNG is real.

IV. Epsilon negative (ENG) media is defined as a medium with permittivity less than zero ($\varepsilon(\omega)<1$) and permeability greater than zero ($\mu(\omega)>1$). Plasmas are a common example of this type of medium. Plasma shields the interior of a field from electromagnetic radiation, and all electromagnetic waves inside the plasma dissipate at frequencies below the plasma frequency. The dispersion relation, which reduces to $k^2 < 0$ in this case, expresses this directly. There is no true solution for the wave vector inside an ENG medium like this. Some dielectric materials, such as SiC, can exhibit ($\varepsilon(\omega) < 1$) across a short frequency band above the resonance frequency due to Lorentz dispersion near an emitter or optical phonon resonance.

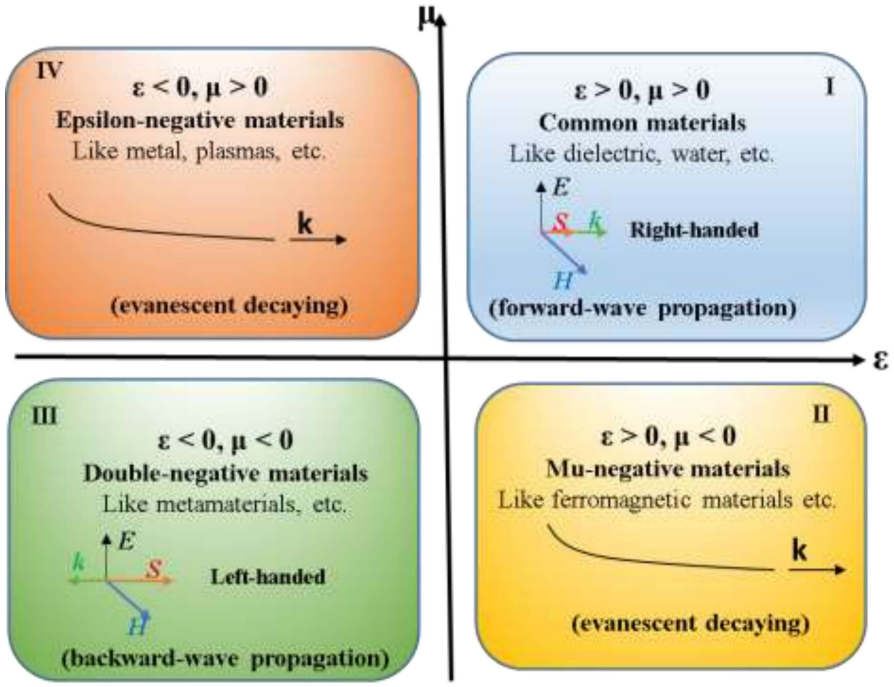

Fig. 1.1 Propagation of electromagnetic waves in materials with different values of permittivity (ε) and Permeability (μ).

1.4 Maxwell's equations: Interaction of electromagnetic waves with materials

Maxwell's equations in an isotopic medium can help us better understand how light, radiation, and matter interact. The following equations show the influence of the signs ε and μ on the interaction of light waves with the matter, as well as the material's propagation properties. Maxwell's equations are represented in the differential form with respect to,

$$\vec{\nabla}.\vec{D} = 0 \tag{1.4}$$

$$\vec{\nabla}.\vec{B} = 0 \tag{1.5}$$

$$\vec{\nabla} \times \vec{E} = -\frac{\partial \vec{B}}{\partial t} \tag{1.6}$$

$$\vec{\nabla} \times \vec{H} = \frac{\partial \vec{D}}{\partial t} \tag{1.7}$$

Where $\vec{D}$, $\vec{B}$, $\vec{E}$, and $\vec{H}$ are represents the electric displacement or electric flux density (C/m^2), magnetic flux density (T or Vs/m^2), electric field (V/m), and magnetic field (A/m).

Electric flux density ($\vec{D}$) and magnetic flux density ($\vec{B}$) in a homogeneous isotropic medium can be calculated using the following equations,

$$\vec{D} = \varepsilon\vec{E} \tag{1.8}$$

$$\vec{B} = \mu\vec{H} \tag{1.9}$$

In an isotopic media, Maxwell's equations can be rearranged as shown in the equations:

$$\vec{\nabla}.\varepsilon\vec{E} = 0 \tag{1.10}$$

$$\vec{\nabla}.\mu\vec{H} = 0 \tag{1.11}$$

$$\vec{\nabla}\times\vec{E} = -\mu\frac{\partial\vec{H}}{\partial t} \tag{1.12}$$

$$\vec{\nabla}\times\vec{H} = \varepsilon\frac{\partial\vec{E}}{\partial t} \tag{1.13}$$

When the electric and magnetic fields are specified in relational terms for a planar monochromatic wave,

$$\vec{E}(\omega,\vec{k}) = \vec{E}_o\, e^{i(\vec{k}\vec{z}-\omega t)} \tag{1.14}$$

$$\vec{B}(\omega,\vec{k}) = \vec{B}_o\, e^{i(\vec{k}\vec{z}-\omega t)} \tag{1.15}$$

Maxwell's equations can be rearranged with the help of Eqs. 1.14 and 1.15,

$$\vec{k}\times\vec{E} = -\frac{\omega}{c}\mu H \tag{1.16}$$

$$\vec{k}\times\vec{H} = \frac{\omega}{c}\varepsilon\vec{E} \tag{1.17}$$

Where ω, $\vec{k}$, and c represents the angular frequency, wave vector of an EM wave, and the speed of light, respectively.

The complex ε and μ values presented in Eqs. 1.18 and 1.19 have a significant impact on the material properties[7].

$$\varepsilon(\omega) = \varepsilon'(\omega) + i\varepsilon''(\omega) \quad (1.18)$$

$$\mu(\omega) = \mu'(\omega) + i\mu''(\omega) \quad (1.19)$$

These values vary depending on the frequency. This indicates that the response alters with frequency.

The index of refraction, as stated in Eq. 1.20, can be used to determine a substance's optical reactivity. The real part of the index is *n*, while the imaginary part is $\vec{k}$ in this relationship. Metamaterials display native values for this relationship that aren't found in natural materials. A substance's index of refraction can alternatively be expressed as a complex function ($\tilde{n}$), such as,

$$\tilde{n} = n + ik \quad (1.20)$$

For a planar monochromatic wave in an isotopic medium, $\vec{E}$, $\vec{H}$, and $\vec{k}$ are always perpendicular to one another and $\vec{E}$ and $\vec{H}$ are in phase, as shown in Fig. 1.2. It is clear that simultaneous changes in ε and μ have an impact on the signs of Eqs. 1.16 and 1.17. Poynting vector ($\vec{S}$), wave vector ($\vec{k}$), electric field ($\vec{E}$), and magnetic field ($\vec{H}$) are geometrically depicted in Fig. 1.2(a) and 1.2(b). Eqs. 1.16 and 1.17 remain unchanged for "Right-hand material" if ε and μ are both positive signs. While both signs of ε and μ are negative at the same time, both Eqs. 1.16 and 1.17 become "Left-handed material". Eq. 1.21 can be used to mathematically explain the behavior of electromagnetic waves traveling in the right- and left-handed materials which demonstrated the energy flux/pointing vector and the wave vector, as shown in Fig. 1.2(a) and 1.2(b).

$$\vec{S} = \vec{E} \times \vec{H} \tag{1.21}$$

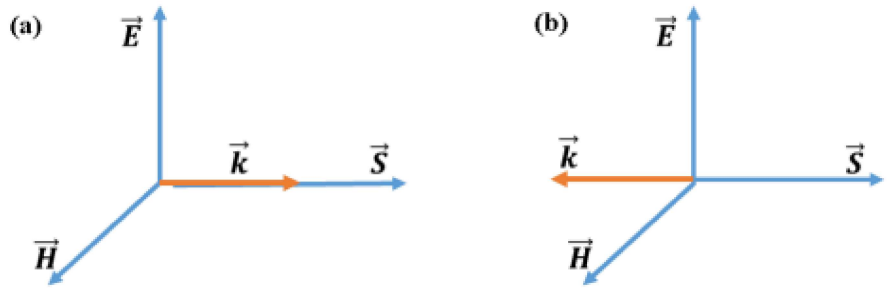

Fig. 1.2 $\vec{S}$, $\vec{E}$, $\vec{H}$ and $\vec{k}$ are geometrically represented in **(a)** materials for right-handed people, **(b)** materials for left-handed people.

$\vec{S}$, $\vec{E}$, and, $\vec{H}$, must all follow the right-hand rule in electrodynamics, and energy must move along the wave vector in the same direction, according to Eq. 1.21. The two vectors ($\vec{S}$ and $\vec{k}$) propagated in opposing directions in the left-hand material, on the other hand. Consequently, because the vector indicates the phase velocity direction, energy flows in the opposite direction as the left-handed material has phase velocity. Left-handed materials are referred to as "negative group velocity materials"[5].

1.5 Snell's law

Snell's law is mostly used to explain how a wave's angle of incidence and angle of refraction change as it passes through various mediums[10]. This law is appropriate for left-handed medium structures. As we saw in the previous section, the phase velocity is negative for wave propagation in a left-handed medium, which has important implications.

Let us take a look at the scattering of the wave formed at the DPS-DNG interface in Fig. 1.3(a) and 1.3(b). Fig. 1.3(a) illustrates the positive index media of the refractive wave traveling through the opposite medium, whereas Fig. 1.3(b) illustrates the negative

index media of the refracting wave traveling through the opposite medium[11]. Its angle of refraction is negative because it is moving backward.

Snell's Law of Reflection states that the angle of reflection is equal to the angle of incidence. By using boundary conditions, Snell's law is produced. The law is expressed as follows:

$$n_1 \, \mathrm{Sin}\theta_i \; = \; n_2 \, \mathrm{Sin}\theta_t \tag{1.22}$$

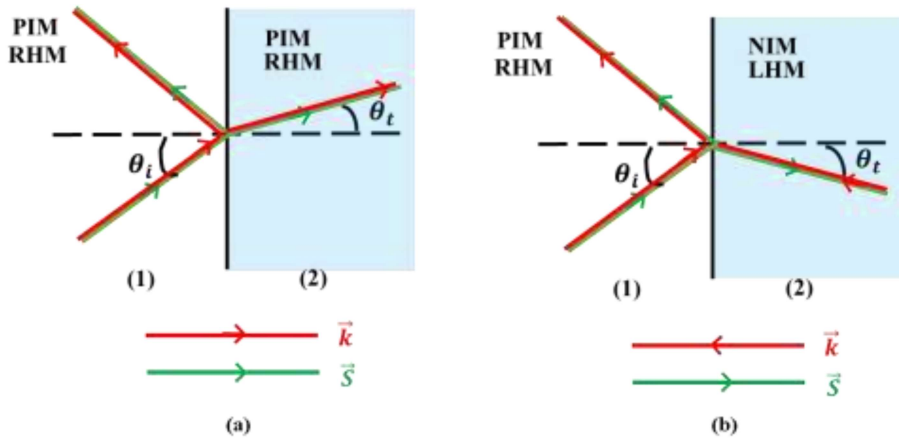

Fig. 1.3 Electromagnetic wave refraction at the interface between two mediums. **(a)** positive refraction in the first scenario involves two media with the same handedness (either RHM or LHM), **(b)** case of two differently handed media (one RHM and the other LHM): negative refraction.

As illustrated in Fig. 1.3, the angles of incidence and refraction are represented by θ_i and θ_t, respectively, while the differing medium refractive indices are shown by n_1 and n_2. If we now take into account the scenario depicted by the former, which has a DNG material with a negative refractive index n_2, we can see that to get the proper angle of the transmitted wave, we need to express the equation as will need:

$$\theta_t \; = sin^{-1}\left[\frac{n_1}{|n_2|} Sin(\theta_i)\right] \tag{1.23}$$

It is important to note that, under Snell's law, if the index of refraction of a medium is negative, the angle of refraction must also be negative. In this case, as we saw in the

previous section, the direction of the energy flow, determined by $\vec{S}$, is the polar opposite of the direction of wave propagation ($\vec{k}$), and therefore opposite. It is also crucial to remember that, because we are working with passive media, we are taking the solution where $n'' > 0$, as we discussed in the previous section. A very important difference was, as we mentioned earlier, that the energy flow was then propagating in the direction of the interface (and the source), which is opposite the causal direction and makes no sense for inert media. However, if we choose to use $n''<0$, according to Snell's law, we will not have a negative refracted angle, but a positive one.

1.6 Negative permittivity and permeability medium

Negative permittivity (ε) and negative permeability (μ) can be realized individually in left-handed materials[12]. There are negative permittivity materials in nature, as was covered in section 1.3. All metals, for example, exhibit negative ε(ω) up to the plasma frequency (ω_p) for the plasma medium. However, because the absolute value of negative is very high at the target frequency, that is, from microwave to optical frequency, the use of solid metal in LHM is constrained. As a result, a strategy for scaling the value to a suitable value on the order of -1 must be developed. The negative value of the permittivity can be calculated using a suitable method using the Drude model[13] which has plasma properties.

$$\varepsilon(\omega) = 1 - \frac{\omega_p^2}{\omega(\omega + i\omega_c)} \tag{1.24}$$

where the ω_c symbol represents the damping frequency and the plasma frequency (ω_p) is given by:

$$\omega_p^2 = \frac{ne^2}{\varepsilon_o m_{eff}} \tag{1.25}$$

where, *n, e*, and m_{eff} symbols represent the electron density of the structure, the electric charge, and the effective mass of free electrons, respectively.

Metals have very high plasma frequencies; for instance, silver has $\omega_p = 2\pi \times 2184$ THz and $\omega_c = 2\pi \times 4.35$ THz. Because of this, the absolute value of permittivity, $\mathrm{Re}(\varepsilon) < -10^8$, is quite high and unsuitable for left-handed materials. Pendry presented a wire array concept that can drastically lower the plasma frequency and achieve negative permittivity $\varepsilon \approx -1$ at microwave frequencies. Additionally, the geometrical parameters allow for total control over the frequency and permittivity value. The wire array arrangement in Fig. 1.4(a) is made up of "infinite" long wires that are organized at regular intervals and have a spacing and radius (*r*). Although the plasma frequency is substantially lower, the effective permittivity of wire arrays is comparable to the permittivity in bulk metal. The real component of permittivity, $\mathrm{Re}(\varepsilon)$, is negative under the plasma frequency (ω_p) as illustrated in Fig. 1.4(b), which is in the range suitable for left-handed materials.

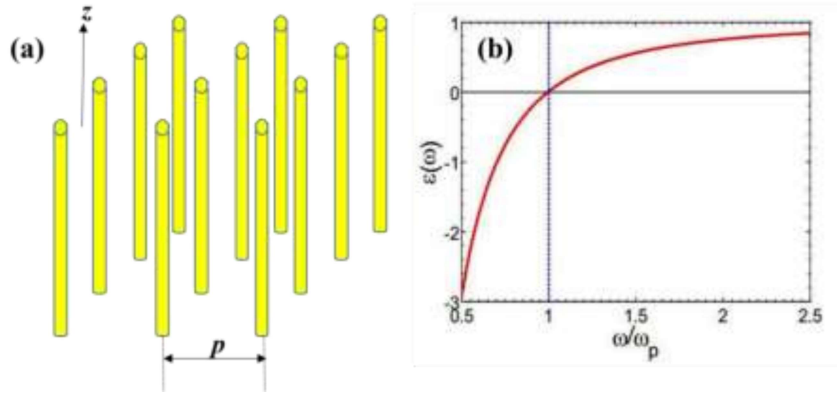

Fig. 1.4 (a) The metallic thin wire array with a lattice period (*p*), **(b)** the real part of the permittivity ($\mathrm{Re}(\varepsilon)$) increases with frequency (ω/ω_p).

The plasma frequency of the wire array is decreasing as a result of two factors. The volume occupied by the metallic thin wire is substantially smaller than the vacuum space,

which results in a large reduction in the effective electron density. Using the formula $n_{eff} = nr^2/p^2$, one may determine the effective electron density by dividing the volume of the metal by the volume of the vacuum. The electrons' velocity, on the other hand, slowed down as a result of the thin wires' self-inductance. The effective mass of electrons grows significantly as a result of the magnetic field energy, which is equivalently proportional to *ln(p/r)* and corresponds to this self-inductance. The ω_p of the wire array is substantially lower than for the bulk metal when these two effects are combined. The wire array's plasma frequency is denoted by,

$$\omega_p^2 = \frac{2\pi c_0^2}{p^2 \ln(p/r)} \tag{1.26}$$

It is clear that the lattice constant (p) and the wire radius (r) are the only two variables that affect the plasma frequency. One can alter the ω_p and subsequently the permittivity value by adjusting these geometrical factors.

Although plasma mediums like metallic structures can acquire negative permittivity, one cannot create a negative medium because there is no material in nature with negative $\varepsilon(\omega)$. Pendry used a split ring resonator (SRR) to attain negative permittivity in the fixed polarisation of incident electromagnetic waves within a narrow frequency range[14]. The SRR arrays, as seen in Fig. 1.5, are made up of arrays of double split ring structures that are built of good conductors like copper and have the lattice constant (p). An electromagnetic wave enters the SRR as it enters the magnetic field, where it is stored and induced currents in the inner and outer metal conducting rings as well as the splitting gap. As a result, a single SRR functions as a series of inductance, resistance, and capacitance (LRC) between the two rings.

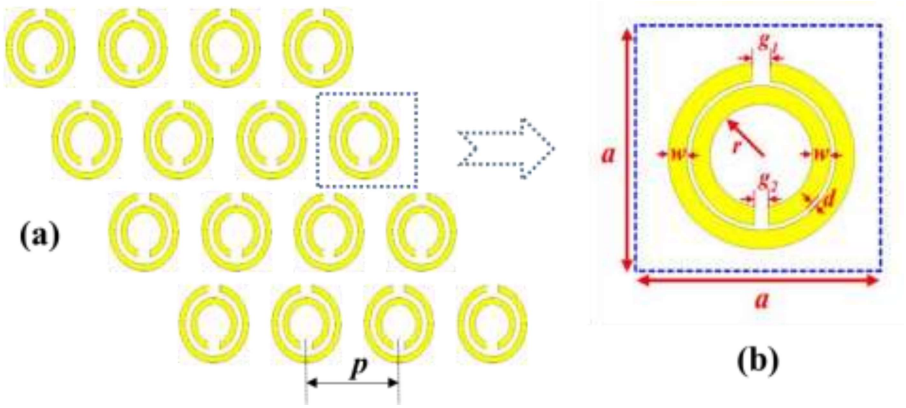

Fig. 1.5 The split-ring structure (SRR) conceptual diagram with repeating distance (p) suggested by Pendry et al., **(b)** SRR single unit cell having the following geometric parameters: inner ring radius (r), ring width (w), inner and outer ring gap (d), and inner and outer ring gap (g_1 and g_2).

The following formula is used to calculate the effective permeability (μ_{eff}),

$$\mu_{eff} = 1 - \frac{A\omega^2}{\omega^2 - \omega_m^2 - i\omega\gamma_m} \tag{1.27}$$

Where, $\omega_m = \frac{3pc_0^2}{\pi \ln\frac{2\omega}{d} r^3}$ $A = \frac{\pi r^2}{p^2}$, and $\gamma_m = \frac{2p\sigma}{r\mu_0}$ symbols represent the resonance frequency, area, and damping factor, respectively. The SRRs array's effective permeability is depicted as a function of frequency in Fig. 1.6. Within a constrained range of frequencies above the resonance frequency (ω_m), negative values of permeability are attained.

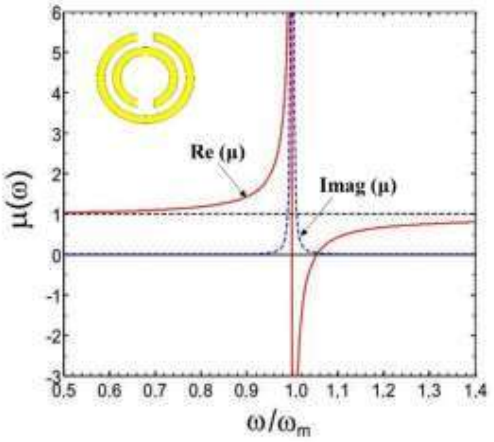

Fig. 1.6 The imaginary and real parts of permeability represented by blue dashed and red solid curves are functions of the frequency (ω/ω_m).

1.7 Materials' electronic properties

Metamaterials (MTM) are engineered materials composed of a series of artificial unit structures (metal molecules/metal atoms) made from pre-existing materials and placed in periodic patterns. The combination of such unit structures in a new material has qualities that are unique from its primary components. As a result, the MTM unit cell determines the response and behavior of a metamaterial structure to an electromagnetic wave (arrangement of composite materials in a unit cell). As a result, while constructing MTM, the / Insulators, semiconductors, and metals/ conductors are the three categories of materials to utilize and their physical qualities (optical and electronic properties) must be carefully evaluated to choose the best material for the desired design, wavelength range, and application. Dielectrics are used in electronics. The conductivity characteristics of these materials are explained by electronic energy levels or energy band structure[13], which are the basis for these classifications. Every material has two primary energy bands: valence and conduction, separated by a space on the electronic scale. The conduction band is normally empty and has the highest energy, while the valence band is partially filled with electrons and has the lowest energy. The "forbidden band" or "bandgap" which represents the empty region between the valence and conduction bands, is critical to the material's conductivity. The electronic energy levels of conductors, semiconductors, and insulators are schematically shown in Fig. 1.7. The conduction band and the valence band are overlapping in metals/conductors. As a result, electrons can quickly jump from the valence band to the conduction band (metals are good conductors of electricity) with only a slight electric field (small biased voltage). Since the bandgap of semiconductors is larger than that of conductors and less than that of insulators, a large electric field is required to move electrons from the valence band to the conduction band in semiconductors. In comparison to the other two, dielectric has a large bandgap. As a result, electrons are unable to do so,

and it takes a lot of energy to leap the empty gap between the valence band and the conduction band, preventing the dielectric from allowing electric current to flow (poor conductor of electricity).

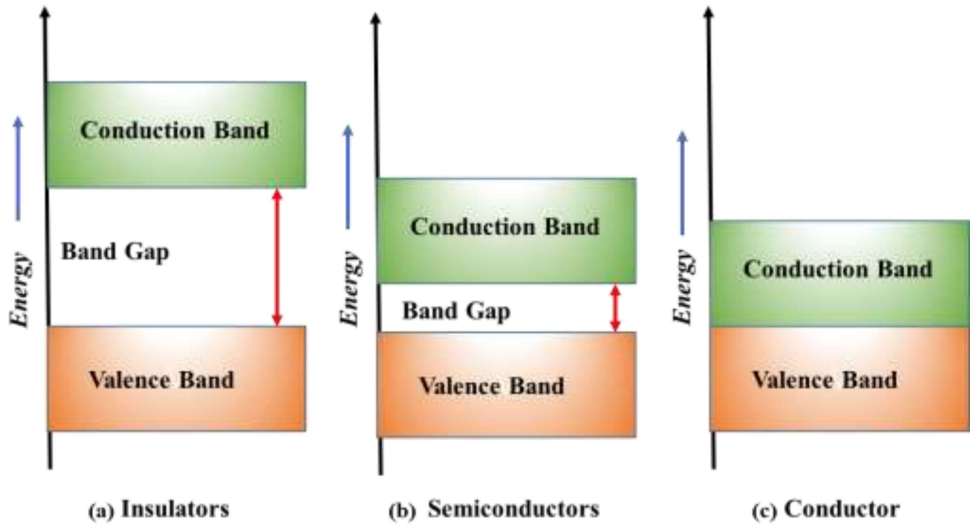

Fig. 1.7 Diagram of the energy band gap for conductors, semiconductors, and insulators. The energy band gap is shown by the distance between the conduction and valence bands[13].

1.8 Metal and dielectric's optical properties

Metamaterials are man-made materials that are created artificially by arranging metal and dielectric unit structures in a periodic pattern. It is important to understand the properties and their physical structure before designing metamaterials. In general, dielectric materials are widely employed in the optics industry for the manufacture of several optical devices. This is due to the important role of dielectric materials in successfully managing electromagnetic wave propagation paths. The dielectric constant of each dielectric material is described in the previous section of this chapter by relations Eqs. 1.8 and 1.9. It is preferable to employ a dielectric that is transparent in this frequency range when developing a metamaterial for optical frequency; failing to do so results in a significant loss of resonant photons in the dielectric, which lowers the metamaterial's performance. The Helmholtz–

Drude model[13], which may be represented by the following equation, can be used to characterize the dielectric constant as a function of frequency.

$$\varepsilon(\omega) = \sum_i \frac{S_i \omega_i^2}{\omega_i^2 - \omega^2 - i\omega\gamma_i} \tag{1.28}$$

Where, ω_i, S_i, *and* γ_i represent the resonance frequency, damping constant, and strength of i^{th} mode, respectively. Contrarily, metals are less frequently used in optical components than dielectrics, but they are crucial in MTM technology. Because they are connected by a dielectric material, the electromagnetic properties of electronics can be influenced (MTM-based devices). They are some of the crucial components that should be carefully examined while selecting appropriate metals in the process of constructing MTMs for optical or visible frequency applications, similar to dielectric materials. The wavelength of the slanted electromagnetic wave affects the metal substrate's reactivity at all times. Let's take an example. The transmittance of specific metals is high when the reflection coefficient of the majority of metallic elements is high (low transmittance). Unless the contact medium's thickness is substantially smaller than the "optical penetration depth/ skin depth" these types of metals will not allow transmission or diffusion of the electromagnetic wave[15]. Metals' reactions and features are caused by the nature of their electron energy levels, as shown in Fig. 1.7. Any incoming radiation striking the metal's surface is sufficient to excite electrons from the valence band to the conduction band since the metal's valence and conduction bands overlap. As a result, before traveling very great distances, all light capable of interacting with the metal layer is absorbed (disappeared) (mostly 10 nm and about 50 nm in a visible range). The dielectric function can be used to explain the physics behind the interaction of light and metal, just as it can for dielectric materials. The unrestricted mobility of electrons inside a metallic crystalline lattice greatly influences the magnetic characteristics of metals. In this case, the Lorentz harmonic model is extended to

metal, with the electrons traveling independently within the metal lattice and with no restoring force to bring them back. The resonance frequency in this case (conventional Lorentz Model) is zero. For the motion of electrons in metals, the "Drude free electron model" is often used, as shown in Eq. 1.29, where electron motion is always related to the incident electric field.

$$\mathrm{m}\frac{\partial^2\vec{r}(t)}{\partial t^2} + \mathrm{m}\gamma\frac{\partial\vec{r}(t)}{\partial t} = -\mathrm{e}\overrightarrow{E_o}\, e^{-i\omega t} \tag{1.29}$$

Where, e, γ, m, $\vec{r}$, and ω symbols represent the charge of an electron, the damping constant, the mass of an electron, the electron's shift from its starting position, and angular frequency, respectively. The displacement vector can be modified by using algebraic adjustments to obtain,

$$\overrightarrow{r}(\mathrm{t}) = \frac{\mathrm{e}\,\overrightarrow{E_o}\, e^{-i\omega t}}{m(\omega^2 + i\omega\gamma)} \tag{1.30}$$

The dielectric function relation for metals can be expressed, using Eqs. 1.8 and 1.30,

$$\varepsilon(\omega) = 1 - \frac{\omega_p^2}{\omega^2 + i\omega\gamma} = 1 - \frac{\omega_p^2}{\omega^2 + \gamma^2} + i\,\frac{\gamma\omega_p^2}{(\omega^2 + \gamma^2)\omega} \tag{1.31}$$

Where ω and ω_p are the electron and plasma frequencies, respectively, at which the electron charge density oscillates. The plasma frequency is determined by the following equation,

$$\omega_p = \sqrt{\frac{ne^2}{m\varepsilon_o}} \tag{1.32}$$

Where, ε_o and n represent the permittivity of free space and the total number of electrons per unit volume, respectively.

Only free electrons are considered in the Drude model (Eq. 1.31), however, some of the electrons in metals are bonded, so not all of them are free. Although most metal characteristics are heavily reliant on free-electron reactions. When working with visible and other high frequencies, the contribution of bound electrons must be considered. The typical Lorentz model, which includes the concept of bound electrons, is written as,

$$\varepsilon_{ib}(\omega) = 1 + \frac{\omega_d^2}{\omega_o^2 - \omega^2 - i\omega\gamma} \tag{1.33}$$

Where, ω_o, ω_d, and γ are representing the oscillation frequency, density, and damping factor of a bound electron at an applied electric potential, respectively. The following relationships lead to the final Drude model of metals with free electrons and interband-bound electrons:

$$\varepsilon(\omega) = \varepsilon'(\omega) + i\varepsilon''(\omega) = \varepsilon_{ib}(\omega) + 1 - \frac{\omega_p^2}{\omega^2 - i\omega\gamma} \tag{1.34}$$

Furthermore, the dielectric function of both low- and high-frequency EM waves is affected by the interband transition. In this scenario, the term $\varepsilon_{ib}(\omega)$ with Eq. 1.34 must be changed by ε_∞ when working at low frequencies far from interband resonance.

$$\varepsilon(\omega) = \varepsilon'(\omega) + i\varepsilon''(\omega) = \varepsilon_\infty - \frac{\omega_p^2}{\omega^2 + \gamma^2} + i\frac{\gamma\omega_p^2}{(\omega^2 + \gamma^2)\omega} \tag{1.35}$$

An in-depth discussion of the experimental results, measurements, additional metal optical properties, and hypotheses is provided in[13,16–18].

1.9 Metamaterial applications

Metamaterials have a wide range of potential applications due to their intriguing electromagnetic properties in electromagnetic research domains such as energy harvesting, optics, and the communications sector. Compact metamaterials can be made with the help of improved manufacturing techniques. This results in less space required and thus lower material cost. Because of their tremendous capacity to manipulate light, these materials could have a bright future in the solar energy industry. This section discusses the medium of various real-world applications of metamaterials.

(1) Invisible Cloak

When metamaterial is used in the invisibility cloak, it is called metamaterial cloaking. The development of the invisible cloak is the first application of metamaterial (MTM). The metamaterials (MTMs) concept can regulate EM fields, resulting in a breakthrough known as the "invisible cloak." Pendry and his colleagues proposed the first entirely invisible cloak based on light bending and coordinate transformation[19]. To do this, a unique optical substance is used to manipulate the directions that light takes. Specific sections of the light spectrum are directed and controlled using metamaterials, which show the ability of an object to appear invisible. Metamaterial cloaking, which is based on transformation optics, is the term used to describe the technique of hiding something from view by modulating electromagnetic radiation. Closed equipment, such as wearables, automobiles, and military jets, is inhibited or fully prohibited from releasing EM radiation using this approach (like radar and other types of remote sensing equipment). As a result, the object may be hidden in it and may not be known. As a result, the object can be concealed within it while remaining undetected[20–22].

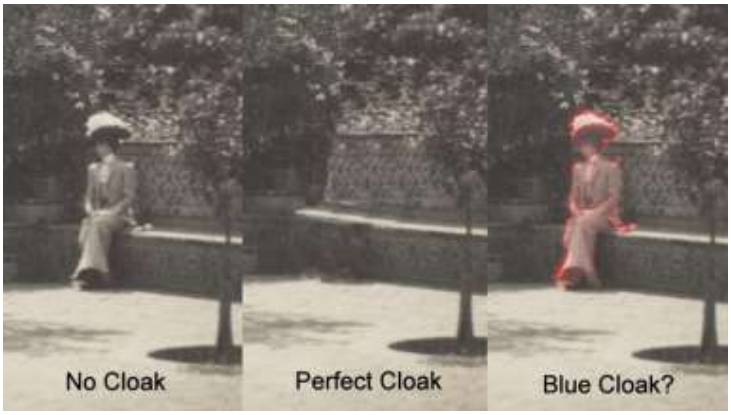

Fig. 1.8 Brian Dodson's image of an invisible cloak (Source: www.google.com).

(2) Sensors

Another potential application of metamaterials is in the development of superior sensors[23–29]. MTMs are employed to provide more sensitive guiding modes based on surface plasmonic resonances. The contact between the metal and the dielectric is where surface plasmons typically form. This phenomenon is greatly influenced by the refractive index of the contact medium as well as the refractive depth of field penetration[30]. The diffusion constant of the surface plasmon changes when the index of refraction of dielectric changes. The features of EM waves linked with the surface plasmon can be altered by applying a few conditions of coupling.

As artificial media with a size scale smaller than the wavelength of external stimuli, metamaterials can display substantial field localization and enhancement, which may offer new tools to significantly improve the sensitivity and resolution of sensors as well as create new design options for them. There are different types of metamaterial sensors that can be utilized for particular purposes[31]. These sensors include wireless strain sensors, thin-film sensors, and biosensors (microwave, terahertz, and plasmonic). Non-invasive blood glucose monitoring is done with a microwave sensor based on a made-

up transmission line. The sensor's dimensions are shown in the corresponding numerical model to have the sensitivity needed for precise blood glucose monitoring[32].

(3) Antenna

A subclass of antennas known as metamaterial antennas makes use of metamaterials to improve the performance of tiny (electrically) antenna systems[33]. They are designed to transmit energy into space, much like any other electromagnetic antenna. Because of its unique structure, a metamaterial antenna acts as if it were much larger than it actually is as it stores and radiates energy. To perform various manipulations on the transmitted and received signals, such as band-pass and band-stop filtering procedures, as well as polarization modification, a wideband horn antenna (laden with particles induced by metamaterials) can be used[34,35]. As a result, the modules can be thought of as a brand-new family of microwave components that perform signal manipulation inside a communication system's radiating element. By utilizing these little modules, we can decrease the number of parts that go into creating a communication system, which has a positive impact on the cost, weight, complexity, and available space[36].

(4) Superlens

Metamaterials could also be used to create superlenses or perfect lenses. Any lens that employs metamaterial to surpass the diffraction limit is referred to as a super lens. Conventional lenses and microscopes have a limit on the fineness of their resolution known as the diffraction limit. A bulk metamaterial-based two-dimensional Lüneberg lens is composed of several concentric layers. By altering the geometric dimensions of unit cells in each layer, the modified Luneburg lens can provide the gradient refractive index profile that is required. In the microwave frequency, the cylindrical waves produced by a point source at the lens' focus might be changed into plane waves as

needed. When the source moves in the lens' circumferential direction, this modified Luneburg lens may perform wide-angle beam scanning. Negative magnetic permeability (μ) and electrical permittivity (ε) as well as MTMs led to the development of superlenses[37]. Professor Sir John Pendry of Imperial College London created the first superlens capable of surpassing the optical diffraction limit using the concept of negative refractive index (n) and MTMs theory[38]. Additionally, both wave propagation and refraction enable the resolution of the images to be below the diffraction limit.

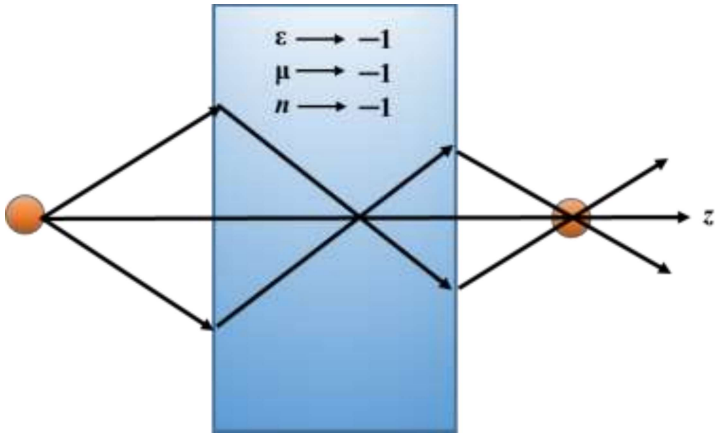

Fig. 1.9 Electromagnetic wave moving in negative refractive index.

(5) Absorbers

The purpose of a metamaterial absorber is to effectively absorb electromagnetic radiation, including light. As development in materials science, metamaterials that are intended to act as absorbers offer advantages over conventional absorbers, such as additional downsizing, a greater range of flexibility, and increased efficacy[39,40]. Perfect absorption is one of the most essential applications of metamaterial structures. To achieve complete absorption, the transitivity and reflectivity of these materials simultaneously must be zero so that all incident EM radiation is absorbed by the material. Even though metamaterial absorbers are composed of multiple layers, they function as an effective material because they are subwavelength

structures concerning the incident wave[41,42]. The properties of a metamaterial absorber are specified by the effective parameters (permittivity and permeability). These specific parameters can be arranged so that the effective impedance of the absorber is equal to the impedance of the free space[43,44]. Under these conditions, perfect absorption can be achieved when the reflected and transmitted waves are reduced to a minimum[45]. Eq. 1.36 can be used to compute the impedance relationship. The geometric dimensions of the structure have a significant effect on the resonant response of the MTM absorber. The metamaterial absorber's electrical and optical responses can be easily tuned by changing these dimensions. Matching impedances can be achieved by carefully adjusting the geometric dimensions of the metamaterial absorber.

$$z(\omega) = \sqrt{\left(\frac{\mu_o.\mu_r(\omega)}{\varepsilon_o.\varepsilon_r(\omega)}\right)} \tag{1.36}$$

Here, μ_o, μ_r, ε_o, and ε_r symbols represent the vacuum permeability, relative permeability, vacuum permittivity, and relative permittivity, respectively.

Furthermore, at high frequencies, plasmon polaritons can generate plasmonic resonances, allowing the incident wave to be entirely absorbed[46,47]. Photovoltaic cells can exploit the perfect absorption capabilities of metamaterials to convert solar energy directly into electrical energy. An active substance is usually needed in a photovoltaic process to collect energy and convert it into useful forms. Light energy is transformed into electron-hole pairs in the active material, which is a semiconductor material. These pairs are then divided into electrodes, from which the energy can be extracted in the form of an electric current. The primary objective

of this thesis is to employ metamaterials to harness solar energy as a renewable energy source.

1.10 Waves at the interface between two media

An ideal metamaterial absorber exhibits double negativity (permittivity and permeability) characteristics and requires certain design specifications (concerning dimensions). It is essential to select the correct material to be used in the design, to determine the frequency range for analysis, as well as the area of use of the absorber. Aside from that, numerical modeling and analysis of metamaterials should be done correctly to ensure that the results acquired are accurate and authentic. As a result, the methods for designing, analyzing, and characterization of metamaterial absorbers are briefly discussed in this section.

Metamaterials have enhanced the absorption coefficients of many devices and have led to the development of novel high-absorption devices. Electromagnetic properties such as electrical permeability ($\varepsilon(\omega)$) and magnetic permeability ($\mu(\omega)$) can be carefully arranged in a metamaterial structure to turn it into a good type of metamaterial structure. The electromagnetic properties of metamaterials depend on geometrical parameters (shape, size, and orientation).

This section will concentrate on the physical processes that can improve the medium's capacity to absorb electromagnetic radiation. Numerous things can happen when an electromagnetic wave interacts with an object. It is possible for electromagnetic radiation to be transmitted, absorbed, reflected, scattered, or refracted. The incident wave may be reflected [$R(\omega)$], transmitted [$T(\omega)$], or absorbed [$A(\omega)$] depending on the surface's average roughness, which must be significantly smaller than the characteristic wavelength to prevent scattering from the roughness. The scattering parameters (S - parameters) are the outputs of the simulation software. The transmission and reflection coefficients can be

calculated using the S-parameters acquired. In general, two primary frequency-dependent parameters define the absorption coefficient (A(ω)) of a metamaterial, as shown in the following relationship. Kirchhoff's rule states that the relationship between the total of transmittance, reflectance, and absorbance must be,

$$A(\omega) = 1 - R(\omega) - T(\omega) \tag{1.37}$$

Using the simulation-derived s-parameters (S_{11} and S_{21}), Eq. 1.37 is simplified as Eq. 1.38,

$$A(\omega) = 1 - |S_{11}|^2 - |S_{21}|^2 \tag{1.38}$$

Where $R(\omega) = |S_{11}|^2$ and $T(\omega) = |S_{21}|^2$ represent the reflection and transmission coefficient, respectively.

Complex amplitude reflections and transmission coefficients can be easily obtained by solving Maxwell's equations inside the surrounding medium and vacuum using boundary conditions from the field continuum. The metamaterial structure must be created in such a way that the imaginary components of their effective ε(ω) and μ(ω) are large enough to eliminate the transmission coefficient. This is because they are the only factors that contribute to metamaterial loss. To negate transmission loss, two methods are widely used. The first method blocks the transmission of electromagnetic waves by combining multiple layers into a metamaterial design. In the second method, the ground plane is used as a metal, where the thickness of the ground plane is much greater than the depth of the skin, which reflects the transmitted wave. Once the transmission losses are eliminated, our sole objective will be to eliminate the reflection rate which remains an obstacle to the achievement of complete absorption. The reflection rate of a metamaterial structure can be reduced by controlling its geometric parameters (shape and size) which depend on the effective properties of the structure (ε(ω) and μ(ω)).

A portion of a plane wave that is traveling through a homogeneous medium and comes into contact with another medium at the interface is reflected off the interface, while the remaining portion of the wave is transmitted. For both transverse electric (TM) and transverse magnetic (TE) polarizations, Fresnel equations that determine the reflectance from a planar contact between materials with (μ_1, ε_1) and (μ_2, ε_2) at an angle from the surface normal are given by,

$$r_{TM} = \frac{\sqrt{\varepsilon_r \mu_r - sin^2(\theta)} - \varepsilon_r cos(\theta)}{\sqrt{\varepsilon_r \mu_r - sin^2(\theta)} + \varepsilon_r cos(\theta)} \tag{1.39}$$

and

$$r_{TE} = \frac{\mu_r cos(\theta) - \sqrt{\varepsilon_r \mu_r - sin^2(\theta)}}{\sqrt{\varepsilon_r \mu_r - sin^2(\theta)} + \mu_r cos(\theta)} \tag{1.40}$$

Where, $\mu_r = \mu_2/\mu_1$, and $\varepsilon_r = \varepsilon_2/\varepsilon_1$ are the relative permeability and permittivity of the two media respectively. Now take into account an air-medium conversation. The reflectance can be determined by assuming that the air side is the normal phenomenon at the interface.

$$\mathrm{r} = \frac{1 - \sqrt{\varepsilon_r \mu_r}}{1 + \sqrt{\varepsilon_r \mu_r}} \tag{1.41}$$

Let's now present the impedance (Z), another optical variable that may be used to characterize the interaction between the magnetic and electric fields, and how it varies as a result of a wave penetrating matter. For a plane wave at position $\vec{z}$, the ratio of the electric field($\vec{E}$) to the magnetic field ($\vec{H}$) defines the load presented to the wave by the medium beyond point *z*. It is possible to further reduce the wave impedance to $Z = \sqrt{\mu_o/\varepsilon_o} = 377\Omega$, which is the impedance of medium 1(vacuum). Now it is possible to express the reflectance

from an interface between two media with characteristic impedances of Z_1 and Z_2, respectively as,

$$r = \frac{Z_2 - Z_1}{Z_2 + Z_1} \tag{1.42}$$

Where, $Z_2 = \sqrt{\mu_2/\varepsilon_2}$ and $Z_1 = \sqrt{\mu_1/\varepsilon_1}$ are the impedances of medium 2 and medium 1 respectively.

The reflectance R(ω) from the medium can be derived from the Fresnel reflection coefficient, which has a complex amplitude.

$$R(\omega) = r.r* \tag{1.43}$$

The reflectance rate of the metamaterial structure can be reduced by modifying these effective properties and also by controlling the structure impedance. The metamaterial structure's impedance matches the free space impedance at the resonance frequency, resulting in a high absorption rate and a very low reflection rate. Since absorption is highly dependent on impedance matching, the impedance of the metamaterial structure can be written as,

$$Z(\omega) = \sqrt{\left(\frac{\mu_o.\mu_r(\omega)}{\varepsilon_o.\varepsilon_r(\omega)}\right)} \tag{1.44}$$

The characteristics of the impedance of free space are,

$$Z_o = \sqrt{\left(\frac{\mu_r}{\varepsilon_r}\right)} = 376.73\Omega \approx 377\Omega \tag{1.45}$$

Where, μ_o and ε_o represent the vacuum permeability and μ_r and ε_r represent relative permeability, and permittivity, respectively.

We conclude from the equations of R(ω) that if the impedance of the medium is equal to the impedance of the surroundings ($Z = Z_o$), then the wave is not reflected through the medium. To be an impedance-matched medium, the effective permeability and the real components of the permeability must be the same ($\varepsilon_r = \mu_r$), thus we get the R(ω) = 0 adjustments, and the absorption is found to be close to unity or unity. Sadly, there is no natural material that can accurately meet these demands. For $\vec{E}$ and $\vec{H}$ to be precisely engineered, one must therefore look to deliberately constructed structures.

1.11 Absorption of light by structured metal surfaces

Electromagnetic absorbers are widely used in devices for electromagnetic energy conversion, temperature detection, and light harvesting. From a microwave to optical wavelengths, these gadgets have an expanding impact on daily life. For instance, microwave absorbers have long been utilized in military applications, EMI reduction, antenna pattern shaping, and radar cross reduction. The terahertz (THz) technology, in contrast, is very new and has a wide range of potential applications in imaging and spectroscopy for biological research and medical diagnostics, high-bandwidth communication, security and defense, and non-destructive testing. Similarly to this, the infrared portion of the light is crucial for thermal imaging, chemical and biological sensing, and other applications. To increase the effectiveness of thin film solar cells and address the energy crisis facing our society, the conversion of sunlight into electricity through the use of light trapping is also of special importance at optical frequencies. It is crucial to note that each of these devices includes absorbers as a necessary component, and a highly absorbing substance is the optimum choice to considerably improve the device's performance.

This section will outline the key ideas behind various EM absorbers as well as the most current developments in metamaterial and plasmonic absorbers. Suppression of the

transmission and reflection must be accomplished to obtain complete absorption of the incident energy. It should be possible for the incident energy to completely dissipate in the medium in question. An optically thick metal layer can be used to provide the zero transmission state. Making a structure with no reflection from the medium's surface is thus one of the key challenges.

1.12 Absorber with anti-reflection coatings

In anti-reflection coatings-based absorbers, a thin transparent film of a carefully selected thickness is deposited over a metal surface in such a way that interference effects in the coating cause the wave reflected from the top surface to be out of phase with the wave reflected from the metal surfaces[48–50]. The optically thick metal layer provides zero transmission conditions. The incident wave is partially transmitted and partially reflected when it hits the front surface of the dielectric. The proportion is defined by the mismatch between the input impedance of the material and the free space's internal impedance; the bigger the mismatch, the greater the reflection. Once this wave has been transmitted, it travels through the dielectric until it reaches the metal support, where it is entirely reflected (in the case of a perfect metal) and travels back to the interface between the dielectric and the air. The same amount of wave energy that was first reflected at the dielectric's outer surface is, in accordance with reciprocity, internally reflected at the dielectric-air boundary, with the leftover pairs being reflected into the surrounding air. When the wave is coupled back into the air, it interferes with the original wave that was reflected at the air-dielectric contact. Between the two interfaces inside the optical cavities, this process is repeated several times, with a small amount of light escaping out at each bounce. The dielectric surface's reflection of light interferes (both constructively and destructively) with the light reflected from the anti-reflection layers. The possibility of phase reversals in the numerous

reflections of light between the two interfaces within the optical cavities by the dielectrics film and the optical path difference (OPD) between the two beams are the foundations for the destructive interference effects. The reason for the phase reversals is that the wave experiences a phase change of radians upon reflection since the metal plate is a perfect electric conductor and has a reflection coefficient of -1.

Fresnel's formula for the reflection of light from a single dielectric film on metal can be used to determine the necessary thickness and refractive index for zero reflection of a dielectric film placed on metal. When light with a free-space wavelength of λ_o is incident on a transparent material with a refractive index of 'n' coated on a perfectly conducting material, the thickness (d) which results in the least amount of reflection is determined as follows[51]:

$$\mathrm{r} = \frac{r_1 + r_2 e^{(-2i\delta)}}{1 + r_1\, r_2 e^{(-2i\delta)}} \tag{1.46}$$

Where δ is the phase difference between the reflected waves, and r_1 and r_2 are the Fresnel reflection coefficients at the air-film interface and film substrate (metal), respectively.

$$\delta = 2\pi nd/\lambda_o \tag{1.47}$$

The zero reflection criterion for a single dielectric contact is satisfied when $nd = \lambda_o/4$, as shown by the aforementioned equation. It is crucial to remember that this sort of absorber depends on the destructive interference of numerous reflections via a thin film of the appropriate thickness rather than the precise value of permittivity or the permeability of the bulk layer.

A dielectric thin film or structure was recently used by Kats et. al.[51] to illustrate another sort of planar absorber on a noble metal substrate (Fig. 1.10.). The ultra-thin, highly

absorbing dielectric has a thickness that is less than one-fourth of the wavelength of the light that passes through the dielectric medium. The non-trivial interface phase changes caused by the significant optical attenuation inside the highly absorbing dielectrics were blamed for the light absorption. Since only the bottom of the cavity is near the metal, as seen in Fig. 1.10., they dubbed it an asymmetric FP cavity**.** By depositing a few nanometres thick films of germanium on top of a gold substrate, they have shown in their study instances of this type of absorber operating at visible frequencies. The sample's color switches from light pink to light blue by adjusting the germanium film's thickness between 7 and 25 nm.

1.13 Resonant absorbers

The Salisbury screen is one of the oldest types of absorber that is intrinsically narrow-band[52,53]. The Salisbury Screen consists of a resistive sheet placed at a distance of an odd multiple of $\lambda_o/4$ wavelengths in front of a metal (conducting) backing and usually separated by an air gap. According to transmission line theory, a short circuit in the metal is changed into an open circuit on the resistive sheet via a quarter wavelength transmission line. The sheet resistance is the structure's actual impedance. The short circuit reappears and the true reflection occurs when the gap is half a wavelength. Good impedance matching is when the sheet resistance is 377 ohm/sq, or the impedance of the air. There is a little area (narrow band) of absorption on a Salisbury screen. The air gap can be replaced by a substance having a higher permittivity. By doing this, the necessary gap thickness is reduced at the expense of bandwidth. The Jaumann absorber is created by integrating many layers for improved performance across a wider frequency range. By combining the resistive sheet and the periodic structure to create resistive cell elements, the structure thickness can be

improved. The majority of such absorbers based on interference effects will often have narrow bandwidths and be wavelength dependant (dispersive).

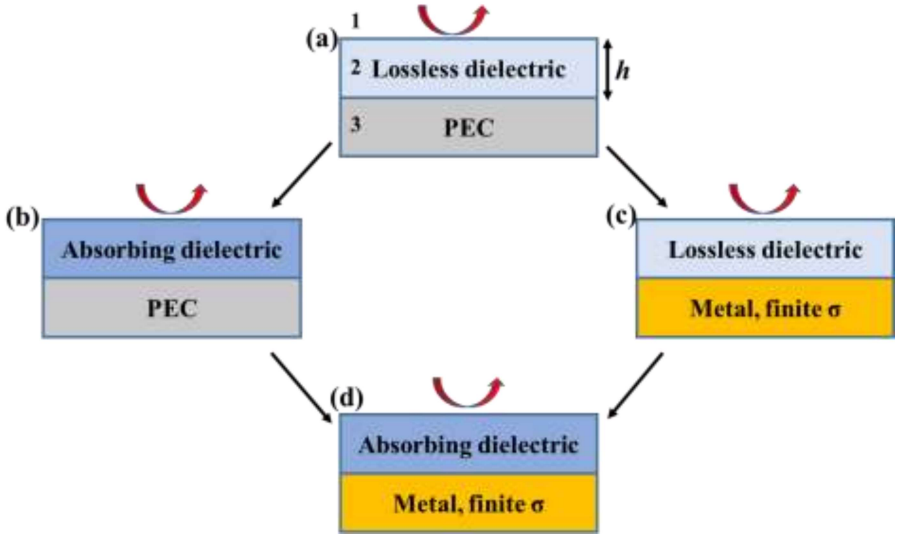

Fig. 1.10 (a) Scenario relating to a lossless dielectric and an ideal electrical conductor (PEC). Since there is neither penetration nor absorption of the metal, the reflectance is equal to one at all wavelengths, **(b**) in the case where the losses are quite small, an absorption resonance is supported by an absorbing dielectric on a PEC substrate, **(c)** the nontrivial phase shifts at the interface between medium 2 and medium 3 can support a resonance in a lossless dielectric on a substrate with finite optical conductivity (for instance, Au at visible frequencies). Still, the total absorption is negligible because the only loss mechanism is connected to the metal's finite reflectivity, **(d)** at visible frequencies, a strong and easily adjustable absorption resonance can be supported by an ultrathin absorbing dielectric on Au[51].

1.14 Surface plasmon-based absorbers

Based solely on visual evidence, Wood[54] proposed in 1902 that a metal grating with an array of metallic components exhibits considerable absorption for specific values of the angle of incidence when a monochromatic plane wave parallel to the magnetic field is generated by its groove at optical frequencies**.** He referred to these experiences as "single anomalies" because he was unable to explain them. In 1907, Rayleigh[55] proposed that the reflection of light passes off at clearly specified wavelengths and used the grating formula to explain Wood's anomaly. The grating duration is the only factor affecting this particular sort of reflection dip. In 1941, Fano made a significant advance in the understanding of

Wood's anomaly. He addressed the fact that, in addition to Rayleigh's conjecture, there exists a forced resonance supported by the particular metallic grating, which results in the reflection valleys enlarging at wavelengths other than those predicted by the grating formula[56]. The entire absorption of light by a metal diffraction grating was demonstrated experimentally and conceptually[57,58] in 1976. Surface plasmon polaritons (SPPs), for short, which are collective oscillations of free electrons supported at the interface between the metal and dielectric, are the primary cause of the physical phenomenon of total light absorption. Later, the same concepts were applied to numerous configurations of various kinds of metal nanostructures, both theoretically and experimentally. Later, these concepts were expanded theoretically and experimentally to encompass a variety of configurations of various types of metal nanostructures[59–61], such as doubly periodic metal gratings[62,63] diffraction gratings made up of cylindrical cavities in a metallic substrate[62], metal-semiconductor-metal nanostructures[64], multi-layers of ordered metallic nanoparticle arrays[65], and partially disordered metallic nanoparticle arrays[66]. The angle of incidence affects the sensitivity of grating-based absorbers. The absorption of localized plasmonic resonances, such as those seen in metallic nanoparticles or nanoslits, is independent of the angle of incidence. To achieve a near unity perfect absorption, it is frequently utilized sub-wavelength metal-insulator-metal (MIM) devices with Fabry-Perot-like resonances.

1.15 Perfect absorber based on metamaterials

The electric permittivity $\varepsilon(\omega)$ and magnetic permeability $\mu(\omega)$ of a perfectly absorbing medium can typically be used to identify it, according to an examination of Fresnel's coefficients. The value and dispersion of the medium's electric permittivity and magnetic permeability must therefore be engineered to achieve perfect impedance matching over a wider range of frequencies[67]. Since many metals exhibit dispersion in $\varepsilon(\omega)$ concerning their

plasma frequency, it is readily available. For the equivalent effect to be reflected in the dispersion of the magnetic permeability, it is essential to build sub-wavelength-sized devices whose resonances can be driven by the magnetic component of the electromagnetic field[14].

In contrast to naturally absorbing materials, artificially structured materials offer robustness and tunability, excellent flexibility to efficiently control and manipulate the absorption of electromagnetic energy, and the ability to engineer effective medium parameters (permeability and permeability) for desired dispersion. A metamaterial's ability to absorb light perfectly is achieved by modifying both the material's electric resonance ε(ω) and the magnetic resonance μ(ω) that results from its structural design. It is conceivable to engineer both the actual and hypothetical parts of and to efficiently absorb incident radiation through both the incident electric and magnetic fields by separately managing these resonances in the metamaterial[68]. The complex permittivity of metamaterials is typically expressed as $\varepsilon = \varepsilon' + i\varepsilon''$. The material's dielectric polarisation produces permittivity. The term "dielectric constant" is occasionally used to refer to the amount ε′, which is somewhat misleading given that ε′ can greatly change (disperse) with frequency. The amount ε″ represents how much the material has attenuated the electric field. A material's electric loss tangent is defined as, $\tan(\theta_e) = \varepsilon''/\varepsilon'$. The attenuation of the wave as it passes through the material increases with the loss of tangent of the medium. The magnetic permeability, which is expressed as $\mu = \mu' + i\mu''$ and has the definition of magnetic loss tangent as follows $\tan(\theta_m) = \mu''/\mu'$, is similar to electric permittivity.

It's crucial to note that increasing absorption is quite challenging. The Fresnel coefficient for the reflection of a wave incoming from a vacuum demonstrates that raising

the imaginary component of the medium's refractive index is not the same as merely increasing absorption. The equation is shown below,

$$R = \frac{n' + i.n'' - 1}{n' + i.n'' + 1} \quad (1.48)$$

Where the medium's refractive index is represented by n' and n" as the real and imaginary components, respectively. Keep in mind that n' + i. n" =$\sqrt{\mu\varepsilon}$. A strongly absorbing media requires n" to be much larger than n'. But as n" approaches ∞, R approaches to take a value of −1. As a result, the material becomes extremely reflective, much like metal is at low frequencies. To obtain perfect absorption, one must be careful to impedance match the medium with the parameters of the surrounding medium.

1.16 Realization of near unity absorbance in metamaterial

The most widely used method for creating a metamaterial absorber structure relies on the simultaneous resonant activation of a magnetic and an electric dipole. A tri-layer system with a top metallic layer organized at sub-wavelength scales makes up the standard design[68]. Due to their substantial resonant enhancement in light scattering or extinction as well as the potential for strong electromagnetic field-enhancing effects in the structures, metal-dielectric-metal nano-sandwiches have been theoretically and experimentally examined in this regard. When the metallic patches that make up the top layer are brought close together, the coupling between the structured patch and bottom metal film induces two types of hybrid modes: a symmetric high-frequency mode where the electric field oscillates in phase in the two metallic patches normal to their axes, and an antisymmetric low-frequency mode where the electric field oscillates with the opposite phase in the two metallic patches normal to their axes. The two oscillation frequencies for the coupled system are similar to those of coupled harmonic oscillators. The symmetric mode with the

in-phase currents in the two nanodisks, as shown in Fig. 1.11 (a), is characterized by a net electric dipole (P). The asymmetric mode is depicted in Fig. 1.11 (b) below as a sum of a magnetic dipole (M) and an electric quadrupole (Q), which results from a current distribution where the currents in the two nanodisks are out of phase[69]. The desired dispersion in the magnetic permeability of the effective medium results from the coupling of the induced magnetic dipole to the external magnetic field. By properly designing the metamaterial structure, one can achieve both magnetic resonance and an electric response at a particular frequency. The engineering of the medium's electromagnetic response depends heavily on each layer of the intended metamaterial. We'll go over each layer's function individually.

The top structural components function as electric resonators powered by the incident radiation's electric field. In the structured unit, the incident electric field stimulates the free electrons' collective oscillation. Because of the structured unit's specific constrained geometry and shape, the excited modes exhibit what is known as cavity resonances. These surface modes exhibit extremely restricted fields close to the margins of metallic structures, allowing for strong coupling to the incident radiation's electric field. The structural unit on top functions as a typical dipole antenna at low frequencies, where metals are almost completely conductive and the skin depth is zero. In this case, the conduction current on the surface of the highly conductive metal patch determines the input impedance. According to the classical antenna theory[70] of resonance at wavelength, $\lambda_{nm} = \frac{2l\sqrt{\varepsilon_r}}{\sqrt{m^2+n^2}}$, where l is the top metallic patch's geometrical length, the permittivity of the surrounding dielectric medium is represented by ε_r, while n and m are positive integers with $m^2 + n^2 \neq 0$. At higher frequencies, however, the antenna's behavior changes qualitatively

when the electromagnetic wave penetrates a significant amount of the entire volume, making the premise that surface currents alone are present invalid.

A recent development that allows us to investigate patch modes both computationally and analytically is the extending of antenna principles from radio frequencies to the visible and infrared regions of the electromagnetic spectrum. Novotny[71] created a straightforward linear scaling law for the expression λ_{eff} given by

$$\lambda_{eff} = n_2 \times [\lambda/\lambda_p] + n_1 \quad (1.49)$$

Where λ_p is the plasma wavelength and, the antenna geometry and static dielectric characteristics are dependent on the coefficients n_1 and n_2, respectively. At wavelengths with resonances, $m*\lambda_{eff}/2 = L$ with $m = 1, 2, 3, 4$, etc., an antenna's length can cause several half-wavelength current oscillations to form. The shaped metal layer may be circular, elliptical, square, rectangular, thin strip (dipole), or any other shape. The most popular configurations are square, rectangular, strip, and circular because they are simple to analyze and make and have well-defined radiation characteristics. These geometries were chosen so that the perfect absorption at microwave and THz frequencies could be demonstrated. The suggested unit may be readily manufactured using well-established printed circuit board (PCB) techniques.

The tri-layer structure's capacitive coupling is significantly influenced by the dielectric spacer layer that is positioned between the top and bottom conducting materials. The electric resonator's resonance frequency can be changed by capacitive loading since, as we've shown, it is dependent on the dielectric characteristics of the top structured layer. This offers a straightforward method of using a tunable dielectric material to tune the resonance of metamaterial. Through inherent dielectric loss, the spacer layer also has a substantial impact on how the absorber radiation is dissipated. At lower frequencies, where

metal is nearly perfectly conducting and metallic structures experience relatively little loss, the absorbed energy must be released in the dielectric spacer material. Based on numerical analyses of the dielectric contribution to absorption at microwave and THz frequencies, it has been determined that the role of the dielectric loss in absorption is significantly greater than that of the ohmic losses in the metal.

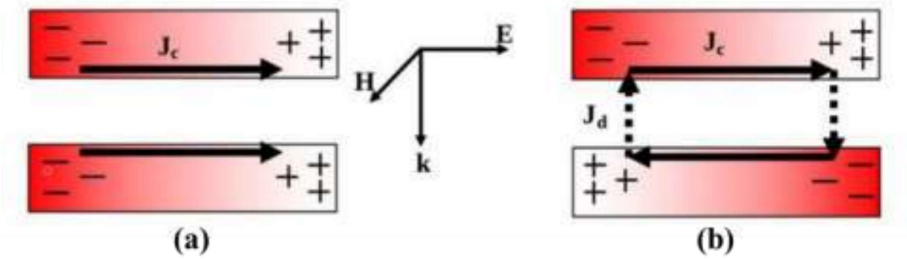

Fig. 1.11 The diagram displays the charge and current distributions of **(a)** the symmetric (electric dipole resonance), **(b)** the anti-symmetric (magnetic dipole resonance).

The best way to explain the ground plane's function is as a perfect conductor that creates the opposite of how charges are distributed in the top structured layer. The oscillating dipoles act as time-varying currents in this instance of time-varying fields. A circulating current loop is made up of two surface currents flowing in opposing directions and the displacement current at the edges. A magnetic field positioned in the perpendicular plane can drive this loop of circulating current. This event causes magnetic excitation, which determines the structure's effective permeability. In antenna theory, the function of the ground plane has been extensively investigated. A ground plane can improve antenna gain by up to 3dB and partially protect objects on the other side by rerouting half of the radiation into the normal direction. A destructive interference with the wave radiated in the opposite direction occurs when the phase of the impinging wave is reversed upon reflection if the antenna is too close to the conducting surface. This is comparable to claiming that there is no reflection since the currents in the antenna and the conductive sheet cancel one

another out. Another type of artificial surface that can serve as a ground plane is one made of a cut-wire metamaterial. The term "ground plane" refers to the portion of a dipole that is above a conducting plane, also known as the Earth's surface, which served as the conducting plane for radio antennas in the past.

1.17 Recent developments in perfect absorber metamaterial

N. L. Landy et al. suggested the first metamaterial-based absorber in the microwave range[72]. As illustrated in Fig. 1.12., the unit cell of the absorber is made up of two unique metallic components: an electric-ring resonator (ERR) on top and a rectangular metal strip on the bottom. These two components are separated by a dielectric spacer layer. The absorber's absorption mechanism is as follows: Electric permittivity is enhanced and dispersed in the top layer of the ERR, which strongly couples to the incident electric field oriented along the ERR resonator's arms. The ERR arms will experience current induction from this time-varying electric field. The metal bar at the base of the dielectric spacer will take on a mirror image as a result of the induced currents in the central arm of the ERR. The displacement currents at the capacitive gap between the dielectric spacer and these two anti-parallel currents create a circulating current loop. Through the circulating current loop, the incident time-varying magnetic field couples to the induced magnetic dipole, producing a magnetic reaction akin to that of Lorentz. The impedance $Z(\omega)$ of the composite medium can be matched to the impedance of free space by adjusting the ERR's geometry and spacer's thickness to match the ε and μ to the ambient medium outside at the same frequency. Second, the ground plane of the metal will not allow electromagnetic waves to pass through, which will likewise result in no transmission. According to Fig. 1.13., the calculated simulated absorptivity $A(\omega)$ at frequency ω_{max} = 11.5 GHz can reach a maximum of 96%. A typical technique for creating metamaterials that operate in the microwave

frequency range, printed circuit board (PCB) technology was used to create the specified metamaterial. Landy et al. were successful in achieving an 88% peak absorption through experimentation. According to the authors, fabrication mistakes were to blame for the differences between simulation and measurement results. To better understand the loss mechanism in the metamaterial structure, the authors also performed a numerical simulation. They discovered that the dielectric loss that occurred between the two layers far outweighed the Ohmic loss and was primarily concentrated in the center of the metamaterial unit cell beneath the strip of the ERR. The narrow-band electromagnetic waves might theoretically be entirely absorbed by the metamaterial absorber.

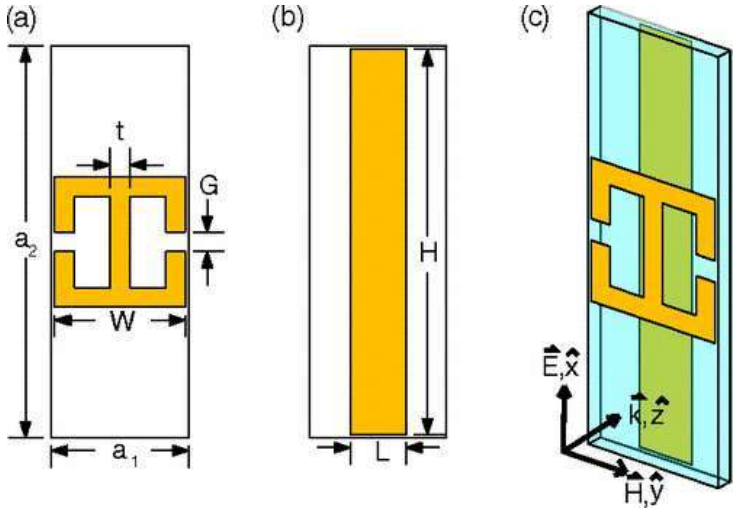

Fig. 1.12 Diagram of a three-layer structure metamaterial absorber **(a)** the layer of metamaterial, **(b)** the bottom metallic layer, **(c)** the unit structure with the dielectric layer. N. L. Landy et al. [72] are the sources for this figure.

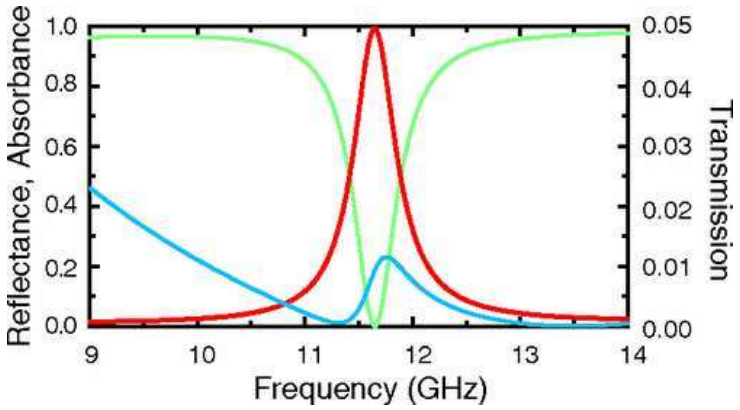

Fig. 1.13 Simulated absorbance for the Fig. 1.12 ideal absorber design for metamaterials. On the left axis, R(ω) (green), A(ω) (red), and T(ω) (blue) are depicted, respectively. Illustration adapted from N. L. Landy et al.[72]

Designs for metamaterial absorbers can be scaled up or down to function at microwaves, THz, infrared, and optical frequencies[73,74]. Simply altering the attributes of each device and the dimensions of the metamaterial structure will do this, depending on the application. Utilizing the downscaling of the microwave absorber design to generate a resonance roughly at 1.3 THz, a comparable design was realized in the THz frequency[75]. The ERR and cut-wire are strongly coupled to the incoming electric field and the magnetic field couples to anti-parallel currents in the middle arm of the ERR and the cut-wire. This is the same absorption mechanism as the original microwave absorber design. The experimental absorptivity of about 70% at 1.3 THz was observed despite the optimal design's simulation predicting an absorptivity of 98% at 1.12 THz. This was caused by the deposited dielectric thickness being less than the optimized one.

1.18 Metamaterials perfect absorber in the different frequency regions

1.18.1 Perfect metamaterial absorber in the microwave frequency

This section will describe several research projects on metamaterial perfect absorbers and their applications in the microwave and THz frequency range.

As already mentioned in this chapter, the first proposed metamaterial absorber structure in the microwave frequency range was prepared by Landy et al.[72]. This absorber could be used to improve image resolution as well as other equipment like the bolometer. Their metamaterial structure's unit cell was made up of two metal layers (cut wire and electric resonator) separated by a dielectric substrate. The electrical coupling was provided by the electric ring resonator, while the magnetic coupling was provided by the antiparallel current in this metamaterial construction. Additionally, the wire from the electro-core resonator touches the wire in a parallel plane that is separated from it by the dielectric substrate. By adjusting the cut wire and the shape of the power resonator, they were able to alter the magnetic resonance of their structure. Their simulation results and experimental results yielded absorption rates of 99% and 88% at 11.65 GHz.

One year later, Costas M.Soukoulis et al. proposed a polarization-insensitive based wide-angle chiral metamaterial (MTM) absorber numerically and experimentally from the University of Crete (Greece) for work in the microwave frequency regime[45]. A grounded metal plane was covered by a dielectric substrate in its metamaterial structures. A split-ring resonator (SRR) that creates an electromagnetic field response was used to cover the top of the dielectric region. For transverse electric (TE) and transverse magnetic (TM) waves, their simulation findings for various polarisation angles (0° to 70°) revealed absorption of more than 90%. The absorption rate for TE waves from the normal 0° to 60° angle of incidence was obtained at 98%. Then, in 2010, Y. Feng et al. proposed a microwave-like polarization modulation technique based on the reflection of a numerically and experimentally metamaterial reflector/absorber[76]. A metamaterial was made by connecting the resonator to the unit cell. By using various modulation signals to control the state of polarization of electromagnetic waves using the geometric characteristics of his design, he was able to control the state of polarization of electromagnetic waves electrically. Their

proposed metamaterial structure was found to be a promising contender for the manufacturing of ellipsometry, VCD spectroscopy, and communications devices. In 2011, J. Zhou et al. proposed an extremely broadband metamaterial absorber based on destructive interference administration for microwave frequency[77]. They generated a suitable dispersion index of refraction by using a multilayer split-ring resonator that can induce continuous antireflection over a wide frequency range. For frequencies ranging from 0 to 70 GHz, they were able to achieve a significant absorption bandwidth of around 60 GHz. Their design could be used in transmission equipment design and optimization, as well as the production of stealth broadband absorbers. In addition, Long Li et al.[78] proposed a dual-band metamaterial absorber for the microwave frequency arrangement. The periodic arrangement of tetra arrow resonators on a dielectric substrate and a metal ground plane was presented in their study. They were able to achieve dual-band with polarization independence at 6.16 GHz and a wide-angle absorber with a 99% absorption rate at 7.9 GHz by adjusting the design of their metamaterial unit cell. Furthermore, multi-band metamaterial absorbance was presented by Y. P. Lee et al.[79]. It was made up of a dielectric substance sandwiched between two ground metal plates with a donut-shaped resonator. Several bands with about 100% absorption rate were found for both TE and TM waves using numerical simulation and experimental verification.

1.18.2 Perfect metamaterial absorber in terahertz (THz) frequency

This section will describe several research projects on perfect metamaterial (MTM) absorbers and their applications in the THz frequency range.

In 2008 Tao et al.[80] proposed the first metamaterial absorber numerically and experimentally in the terahertz frequency regime. This absorber yielded an absorption rate of 98% from numerical simulations at 1.12 THz and an absorption rate of 70% from

experimental characterization. The first narrow-band metamaterial absorbers at THz frequencies were achieved, which are very important keys in the production of thermal sensors. In reference[80], a metamaterial absorber with the ability to have a high absorption rate of 97% at 1.6 THz has been designed, fabricated, and characterized for high flexibility and wide angle of incidence. This created metamaterial showed promise as a nonplanar absorber application material. H-T Chen[81] developed a narrow-band MTM absorber with an absorption rate of around one unit at 1THz using interference theory in 2012. MTM absorber systems with dual-band, triple-band, and broadband responses in the terahertz frequency range[82–84] have also been presented.

1.18.3 Perfect metamaterial absorber in the infrared frequency

Researchers have been able to create metamaterials in the high-frequency infrared (IR) spectrum thanks to continuous improvements in the study of metamaterial absorbers. Padilla et al.[85] created the first metamaterial absorber that completely absorbed an electromagnetic wave in the infrared spectrum. Their metamaterial structure yielded an excellent absorption rate of 97% by numerical simulations and experimentally at a wavelength of 6 micrometers. They used a periodic combination of a dielectric spacer, a cross-metal resonator (ERR), and a ground metal plate (to stop electromagnetic radiation from spreading) to form the structure of the metamaterial. The small magnetic resonance and a highly uniform electric field resonance were caused by the cross resonator. The top cross-resonator metal generates antiparallel currents with the ground plane which generates strong magnetic field resonance. The metamaterial structure was able to match the impedance-free space of this design by adjusting the geometric parameters, thus the proposed design reduces the reflection to a negligible value and achieves almost perfect absorption[85]. Their inventions could be used in hyperspectral subsampling imaging. In 2009, Avitzour et al.[86] presented a research study on infrared metamaterial perfect

absorbers. They were able to achieve a perfect absorption rate of nearly 100% by employing the Anisotropic Impedance Matched technique. Their metamaterial construction produced similar results for infrared light over a wide range of incoming angles, enabling infrared imaging and the production of coherent thermal sources. Metamaterials with various absorption properties and a wide range of applications have been used to accomplish a variety of functions in infrared radiation frequencies[87–90].

1.18.4 Perfect metamaterial absorber in the visible frequency

It has been a challenging task to develop MTM absorbers for the visible spectrum of electromagnetic waves as compared to other frequency ranges. This is because the ability of MTM absorbers to react the incoming electromagnetic radiation is constantly dependent on their effective electrical permeability and magnetic permeability, and the metamaterial structure requires these parameters to fully absorb the incident electromagnetic radiation. As a result, the metamaterial absorber's unit cell must be exceedingly small (subwavelength) when compared to the wavelength. This poses fabrication problems in the visible spectrum because a unit cell must be in the tens of nanometer range. Several applications belonging to this category have been proposed to make metamaterials perfect absorbers in the visual field. Surface plasmon methods, structural gratings, and periodic organization of nanoparticle structures are used to build most metamaterial absorbers in the visible range[91]. The surface plasmon approach achieves the perfect absorption in the visible frequency using localized surface plasmon resonance (LSPR) which results comes from the coupling of the top resonator layer of the metamaterial structure and the ground metal plane. Using surface plasmon technology, Duan et al.[92] suggested a polarization-insensitive based broadband MTMs absorber with an absorbance of about one unit in the visible frequency range. A Kerr dielectric spacer separated two metal sheets (gold) in his metamaterial construction. They were able to remove the radiation losses associated with ground-level

transmission by choosing a ground metal layer with a thickness higher than its skin depth in the visible frequency. To increase absorption, they increased the transmission of the resonators of their unit structure, which was accomplished through two mechanisms: first, the periodic oscillations of subwavelength structures caused by the excitation of surface plasmon polaritons; and second, the LSPR, which is caused by the geometry, size, shape, and orientation of the structure. At the resonant frequency, the MTM impedance coincides with that of free space, and they were able to generate nearly four perfect absorptions using these two methods. The broadband metamaterial unit cell offered potential in the application of solar cells, thermal detector imaging, etc. by Duan et al.[92]. Wu et al.[93] suggested an integrated plasmonic MTM absorber/ emitter for solar energy harvesting in the visible frequency range. In 2014, L. Mo et al.[94] suggested an upgraded broadband absorber. They designed gold absorbers with plasmonic tapered coaxial holes and polarization-independent absorptions in the visible frequency region, both theoretically and experimentally. Furthermore, for wide incident angles for the electromagnetic wave, MTM perfect absorbers with absorption coefficients and wideband absorption while maintaining the same absorption value were presented and explored in mentioned refrerences[95–97].

1.19 Methodology for analyzing

Modeling and characterization of the developed structure using computer simulation software using the finite integration technique (FIT) are presented in this thesis. The frequency-domain solver of the simulation program is used to investigate the frequency-dependent absorption response of the intended structure. In this section, more information on FIT will be provided.

This thesis contains metamaterial absorber designs for solar energy harvesting applications. The solar frequency range, which is between 100 THz and 1000 THz, is therefore chosen

as the frequency range. Under this arrangement, the complete material selection, physical properties, dimensions, and absorption reactions are analyzed. The solar range, on the other hand, has a large frequency range, and different parts perform distinct functions. As a result, some designs divide this broad frequency range into subcategories such as infrared (IR), visible, and ultraviolet (UV), and the proposed structures are studied independently.

To simulate each metamaterial design, suitable boundary conditions are used. In general, the simulation boundary conditions are chosen to be periodic in the x- and y-axis, with the open boundary in the z-axis (lateral direction). The primary unit cell (called a unit cell) is repeated in both the x and y axes by periodic boundary constraints[98]. Along these axes, it produces an infinite lattice of virtual unit cells. Not only is the reaction from the primary unit cell shown, but also the interaction between the primary cell and surrounding virtual cells. Since this thesis not only describes the design of the unit cell of a metamaterial absorber, it is also suitable for virtualizing the optical properties of the unit cell[99].

For all simulations in this thesis, the incident electromagnetic propagation direction is assumed to be in the z-direction. Unless otherwise specified, the transverse electromagnetic mode (TEM) is understood to be the mode of polarization of the incident wave. However, light can be polarized in other modes, such as transverse electric (TE) and transverse magnetic (TM) modes[100]. As a result, the designs are also examined in terms of these modalities. Fig. 1.14. depicts the distinction between these modes. The electric field component is represented by the"$\vec{E}$," while the magnetic field and the incident wave's propagation direction are represented by "$\vec{B}$" and "$\vec{k}$," respectively.

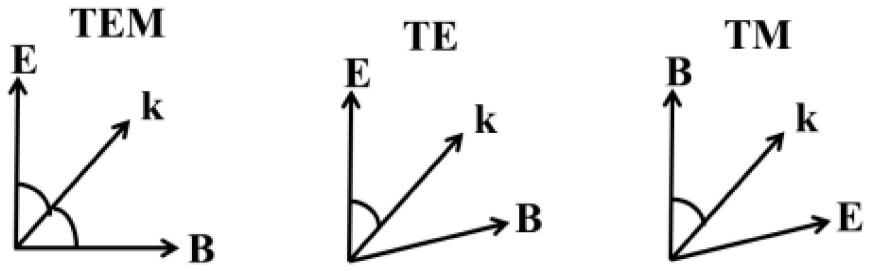

Fig. 1.14 An example of the various wave modes.

Another essential topic to consider is meshing, which is crucial in resolving the electromagnetic problem. The mesh is created when the simulation software separates the proposed structure into little components. The mesh type and mesh density utilized have a direct impact on the accuracy of the results. If the specified mesh density is insufficient to solve the electromagnetic problem, the findings will be inconclusive or wrong[101]. A physics-controlled tetrahedral mesh with adaptive mesh refreshing is employed throughout the thesis. Adaptive mesh refreshing guarantees that the mesh density output is enough for accurate and consistent outcomes. This mesh simulates the structure with an increasing number of cells until the difference between the simulation results is smaller than the chosen accuracy standard.

1.20 Selection of numerical simulation software

The features of metamaterials (MTMs), as well as the key parameters that contribute to their superior properties, were covered in detail in the previous section. The selection of the size, shape and geometric orientation of the appropriate metamaterial (MTM) absorber unit cell is one of the most important steps for the development of suitable MTM absorber structures. This is because the absorption characteristics of an MTM absorber depend more on the geometric nature of its material rather than its chemical composition. In the design of MTM absorbers, the Drude model[13] plays a crucial role. Deciding on the numerical

simulation program to be used for the characterization and design of MTM absorber unit cells is a critical step in the MTM absorber fabrication process. There are many commercial computer software available in the market. Each software metamaterial absorber design approach has its own set of benefits and drawbacks. In this study, a computational program based on the finite integration technique (FIT) is employed for the design and characterization of the suggested metamaterial absorbers. Apart from the FIT technique, there are other techniques available to design the proposed absorber which is based on different types of simulation software.

The choice of a suitable numerical simulation tool to be utilized in the investigation of electromagnetic (EM) field problems is a crucial step. As a result, selecting numerical package software necessitates a thorough understanding of the sort of EM wave problem as well as the frequency range of interest. Memory requirements, geometric modeling accuracy, the numerical solver, and the time it takes for the solver to finish a simulation are all important factors that are taken into account when choosing a software package for electromagnetic field problems. There are many commercially available numerical solvers for modeling electromagnetic wave problems, but each solver has its own set of benefits and drawbacks that vary depending on the type of electromagnetic wave problem to be solved. The finite difference time domain technique (FDTD), finite element method (FEM), modal methods, and finite integration techniques (FIT) are some of the most extensively used approaches for the numerical analysis of electromagnetic[102].

1.20.1 Finite Element Method (FEM)

The finite element method uses numerical analysis to understand approximation solutions to partial differential equation boundary value problems. The continuous domain is substituted by a subdomain (limited element) in this strategy, which employs the

interpolation function to represent the unknown function[102]. FEM's benefits include its high geometric flexibility in modeling curved geometric shapes without uniform material properties, as well as its ease of modification and dynamic nature. The following are some of the disadvantages of this method:

1. As a result of the high memory requirements, finding a viable solver for this method is difficult.
2. Time harmonic Maxwell's equations are difficult to discretize.
3. Computing Maxwell's equations at higher frequencies have limitations when using quick iterative solvers like a flop[102].

1.20.2 Finite Difference Time Domain (FDTD)

Yi[103] devised a Finite difference time domain numerical analytical approach for solving electromagnetic field problems. This method is part of the grid differential numerical modeling methodology that uses finite difference expressions to approximate all temporal and spatial derivatives of time-dependent Maxwell's equations.

The following are some of the benefits of FDTD:

1. Because FDTD is matrix-free, it does not require the use of an iterative solver.
2. This method is simple to use and permits parallel computation, which is critical for faster and more accurate modeling of 3D structures.

FDTD has the following drawbacks:

1. To solve this, you'll need to grid the full computational domain and have enough grid discretization.

2. It requires that the entire computing domain be gridded with sufficient grid discretization to resolve both the smallest EM wavelength and the smallest geometrical structure in the model.
3. As a result, the computation time is extremely lengthy.
4. As a result, this method isn't a better option for computing very small structures.

1.20.3 Finite Integration Technique (FIT)

The finite integration technique approach is based on Maxwell equations. Using this technique, an equation's integral form can be changed into a linear system of equations. For modeling homogenous mediums, this method is good, and it's similar to FDTD[103]. Maxwell's equations (integral form) are converted into a pair of interlocked discretization grids using FIT. i.e., following analysis, the structure is rationalized into mesh cells, which divide the computation domain into several grid cells. The simulation program creates a second orthogonal grid in addition to the first one the computer user developed, and both provide a general description of the system. This mesh is provided by the computer user. After that, the scattering parameters and far-field radiation patterns of the system can be acquired and studied.

This technique is one of the most accurate modeling techniques available, and it's also simple to use. It enables efficient parallel computing and more accurate results when computing complicated designs, as well as being adaptable when it comes to geometric modeling. The method's flaw is that it relies on the Yi Cartesian mesh, which makes computing non-orthogonal complex designs more difficult.

All numerical simulations in this thesis are performed using the FIT approach, which is primarily because it is easier to use and more adaptable. It can be used to model difficulties with 3-D EM wave structures and is suitable for obtaining more accurate results.

Furthermore, numerous researchers have utilized the FIT approach to analyze EM wave problems in serval frequency ranges of the solar spectrum, and it has been demonstrated to produce better findings[102,104–106].

1.21 Geometrical parameters and materials selection

After settling on the right kind of software, another crucial step is choosing the geometric parameters for the proposed metamaterial (MTM) design. Geometric parameters such as shape, size, and orientation play an important role in the study of MTM absorbers. This is because the values of permittivity (ε) and permeability (μ) have a significant impact on the interaction of MTM absorbers with EM waves and their responses. As a result, these characteristics are influenced by the metamaterial structure's shape, size, and, orientation, as well as the wavelength of interest. Consequently, the electromagnetic field in the metamaterial design is determined by resonance ε(ω) and μ(ω). Metamaterials can be defined as properties derived from their geometry rather than their physico-chemical structure. Therefore, when designing a metamaterial structure, the size or average surface roughness of the resonator should always be much smaller than the wavelength[74,107] under consideration ($L<<\lambda_o$). Metal sheets, such as gold, silver, aluminum, lead, copper, and other metals, are used to make resonators that are widely utilized. The metamaterial absorber as a composite structure consists of more than two layers. These consist of a combination of a metal layer and a dielectric spacer. After this, the geometric parameters and suitable material for the resonator are selected and the physical characteristics need to be determined. The ground plane of many metamaterial absorber designs is made up of metal-based materials that help to prevent electromagnetic radiation from escaping into space (transmission loss) by reflecting it back to the dielectric layer. Usually, a metal ground with

a thickness significantly greater than the depth of the skin or the depth of penetration (δ) is used to eliminate these disadvantages.

$$\delta = \frac{c}{\tilde{k}(\omega) \times \omega} \tag{1.50}$$

where ω, c, and $\tilde{k}$ represent the angular frequency, the velocity of light, and the extinction coefficient. Because the primary function of the ground metal is to prevent radiation from returning to space, the dielectric spacer and resonator are the only layers that must be closely monitored once it has been properly selected. The absorption rate can thus be boosted by selecting a lossy material with a good dielectric constant and properly aligning the top resonator with the ground plane, where the impedance of the structure corresponds to the free space impedance ($Z(\omega) = Z_o(\omega)$). In addition, the EM wave frequency range of relevance influences the choice of dielectric material and geometric design. This is because the strengths and weaknesses of each dielectric material vary depending on the wavelength and application. When designing an optical metamaterial, for example, the chosen dielectric material must be transparent to all radiation in the wavelength range in question[13].

1.22 Motivation of the thesis

The energy requirements of human beings are increasing every day. Fossil-fuelled power plants, hydroelectric power plants, and nuclear-fuel-burning power plants are the primary sources of energy for this requirement. The burning of these sources causes harm to the environment, atmosphere, and humanity. This condition has an impact on global temperature as well. The increase in the mentioned greenhouse gases leads to an increase in temperature globally. Furthermore, this growth has the potential to have several negative consequences for the environment as well as human health. Aside from that, price volatility in coal and oil is a problem. Since these sources provide most of the electricity, this situation

can result in a rise in electricity prices. The total estimated energy generation potential of energy resources worldwide can be divided into fossil fuels, nuclear fuels, and renewable resources, given that all assets are available on Earth. On our home planet, some energy sources, such as coal and fossil fuels, are plentiful. Depending on consumption rates, natural gas might meet the majority of the world's energy demand for 100 to 250 years.

Nuclear energy could be one option for avoiding fossil fuels. When compared to fossil-fuel-powered power plants, nuclear power plants produce fewer greenhouse gases in the atmosphere. It is, nevertheless, an environmental hazard. Finally, the Fukushima Daiichi disaster in Japan in March 2011 demonstrated the safety of nuclear power.

Hydroelectricity is a clean source of energy, but it requires a great amount of water to operate and must be situated in the path of this massive volume of water. Renewable energy sources can provide energy demand without releasing greenhouse gases into the atmosphere.

1.22.1 Solar energy

A popular and commonly used energy source is solar energy. This source can be used to supply clean energy using solar cells. Thermo-photovoltaic (TPV) and Photovoltaic (PV) solar cells are two different types of solar cells. Solar cells are unable to convert all solar radiation in the solar spectrum due to their limited solar energy utilization performance.

Fig. 1.15 depicts a sun spectrum map with a wavelength range of 250nm to 2500nm. The plot is divided into three sections: ultraviolet (UV), visible, and infrared (IR). UV C (100 nm to 280 nm), UV B (280 nm to 315 nm), and UV A (315 nm to 400 nm) are the three types of ultraviolet light with wavelengths less than 400 nm. The visible spectrum ranges from 400 to 750 nanometers. The visual spectrum is perceived as seven hues by the human eye (violet, indigo, blue, green, yellow, orange, and red). When IR photons are absorbed

by human skin, they feel like heat radiation. Infrared rays play an important role in determining the temperature of the atmosphere and even the climate of the Earth. The wavelengths of infrared radiation range from 750nm to 1m. Near-infrared is the IR spectrum that is closest to the visible spectrum, whereas far infrared is the longer spectrum.

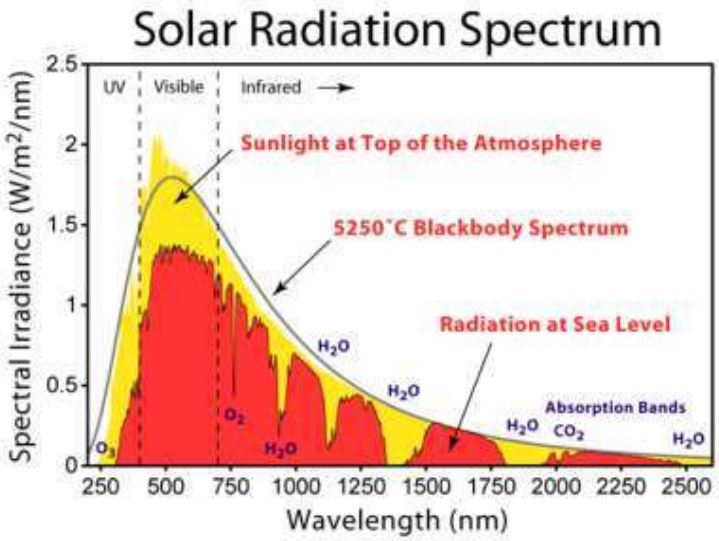

Fig. 1.15 Solar Spectrum (source: www.google.com)

If the losses that contribute to solar cell inefficiency could be reduced, the performance of the solar cells might be further enhanced. Some of these are losses such as optical and recombination losses, aside from the drawbacks, the production and manufacturing costs of a unit cell of solar cells play a crucial role in determining the usage density of these cells. The newly discovered fabrication process paves the way for low-cost unit cell production. The cost of the material can be minimized by distributing it among suitable persons based on the material's availability in nature. Metamaterials could play a key role in reducing losses if the above difficulties are taken into account, we will discuss it in the next section.

1.22.2 Metamaterial absorber

The solar cells' ability to absorb energy has historically been constrained. The capacity to harvest more energy can be determined by the rate of absorption. Numerous initiatives to increase the effectiveness of these solar cells have been made over time. Recently, attempts have been made to increase solar energy absorption and metamaterial (MTM) absorbers have been taken into consideration. It has been demonstrated that metamaterial absorbers are perfect absorbers for solar cell applications. The implementation of an MTM-based perfect absorber with polarization insensitivity for different shapes has been studied for years. Depending on their design and the materials they are made of, these metamaterial structures can absorb visible bands that can be used for photovoltaic energy harvesting applications.

For a single-band, dual-band, and multiband, as well as wide broadband, the MTM absorbers are presented. This MTM absorber adds tunable capability by adjusting the thickness or geometry dimension change. Metamaterial absorbers can be built using a variety of structural methods, including periodic models, resonator constructions, and composite right/left transmission lines. An impedance resonator-based MTM structure is introduced as the top layer to reduce the size of the proposed design. Through parametric analyses, the geometry of the unit cell is tuned to find the best dimensions for a high absorption rate. Furthermore, thanks to advanced manufacturing techniques, these devices may be manufactured as small as possible, allowing them to fit into smaller spaces and operate more efficiently.